

Theory for dissipative time crystals in coupled parametric oscillators

Stuart Yi-Thomas* and Jay D. Sau

Condensed Matter Theory Center and Joint Quantum Institute, Department of Physics,
University of Maryland, College Park, Maryland 20742-4111, USA

(Dated: December 5, 2024)

Discrete time crystals are novel phases of matter that break the discrete time translational symmetry of a periodically driven system. In this work, we propose a classical system of weakly-nonlinear parametrically-driven coupled oscillators as a testbed to understand these phases. Such a system of parametric oscillators can be used to model period-doubling instabilities of Josephson junction arrays as well as semiconductor lasers. To show that this instability leads to a discrete time crystal we first show that a certain limit of the system is close to Langevin dynamics in a symmetry breaking potential. We numerically show that this phase exists even in the presence of Ising symmetry breaking using a Glauber dynamics approximation. We then use a field theoretic argument to show that these results are robust to other approximations including the semiclassical limit when applied to dissipative quantum systems.

The past several years have seen new proposals for possible candidates for phases of matter [1–3], dubbed “time crystals”, that show spontaneous breaking of time-translation symmetry. However, later works [4, 5] showed that continuous time-translation symmetry-breaking was not robust, leading to the focus on “discrete time crystals” (DTCs) in driven Floquet systems which reduce a time-translation symmetry group \mathbb{Z} to a subgroup $n\mathbb{Z}$ [3, 6–11]. While an external drive in a closed system generically results in an infinite temperature steady state, [12–14] disorder and many-body localization in closed quantum systems [3, 7–9, 15–18] and high frequency drives in classical Hamiltonian systems [19–30] may provide possibilities of dynamical symmetry breaking in a finite temperature phase.

Another simpler route, which has been the focus of theoretical [24, 31–35] and experimental works [36–46] in both quantum and classical systems, is to use dissipation to avoid such infinite temperature steady states. Such dissipation may lead to DTC order even in classical systems. While such behavior might appear to be reminiscent of subharmonic entrainment in classical mechanics [35, 47–50], it is unclear to what extent such phenomena are robust to noise as expected in a thermodynamic phase [51]. In the modern context, classical discrete time crystal (CDTC) behavior appears in coupled arrays of nonlinear pendula (e.g. the so-called parametrically-driven periodic Frenkel-Kontorova model) [29, 52], though these systems lack a truly infinite autocorrelation time. Specifically, work by Yao et al. [29] utilizes a strong nonlinearity and finds an “activated” transition where the autocorrelation time grows with temperature. Other models, utilizing probabilistic cellular automata (PCAs), do find infinite autocorrelation times [53–55], even mapping such procedures onto a Floquet Hamiltonian [11], though they have rather com-

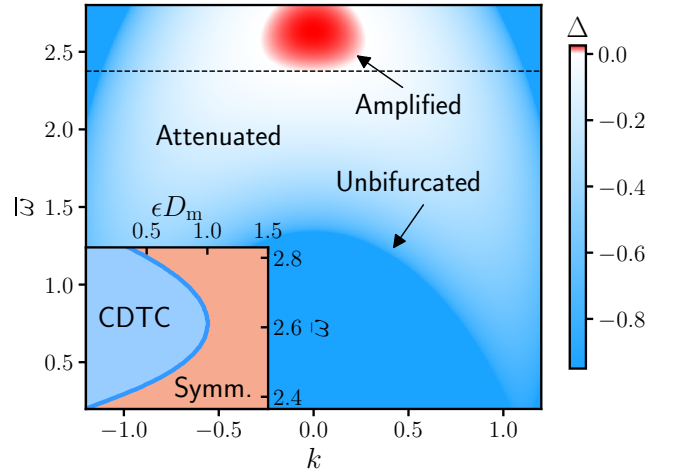


FIG. 1. Total gain Δ of period-doubled state after one period as a function of momentum k and average natural frequency $\bar{\omega} \equiv (\omega_1 + \omega_2)/2$ with damping $\Gamma = 0.95$. The gain is given explicitly by $\Delta = \log |\lambda_k| - \Gamma T$, where λ_k is the largest Floquet eigenvalue of the oscillator by magnitude. All bifurcated points are in the period-doubled regime, i.e. $\text{Re } \lambda_k \leq 0$. The horizontal dashed line corresponds to the point where the damping is critical, i.e. $\Gamma = \Gamma_c = T^{-1} \log |\lambda_{k=0}|$. (inset) CDTC phase diagram in a 2-dimensional weakly-nonlinear parametric oscillator system based on $\bar{\omega}$ and the variance of the microscopic noise ϵD_m . Parameters from Eq. 7 are compared with numerical results from [56]. $J = 10$, $|\omega_1 - \omega_2|/2 = 0.664\pi$, and $g = \nu = T = 1$.

plex physical realizations with several-body interactions.

In this work we propose an absolutely stable CDTC in an array of parametrically-driven perturbatively-nonlinear dissipative oscillators and use this construction to study a CDTC phase. Using a weak nonlinearity, this system exhibits an infinite autocorrelation time in experimentally-tractable system. Similar parametric oscillator systems have been shown to realize period-doubling bifurcations in semiconductor laser systems [57], nanoelectromechanical systems [58] and Josephson junc-

* snthomas@umd.edu

tion arrays [59], all of which can operate in both dissipative quantum and classical limits. As shown in Fig. 1, for an appropriate choice of the average natural frequency, the array of oscillators shows a period-doubled amplifying phase over a small range of wavevectors k .

We show that, for an appropriate choice of weak nonlinearity (relative to previous work [10, 23, 29]) and noise in the classical limit, the above system shows a symmetry-breaking transition that can be described by Ginzburg-Landau theory. The CDTC order features a time scale that scales exponentially in system size, similar to equilibrium symmetry breaking [60–62]. We use a Monte Carlo simulation to demonstrate that this phase is robust to perturbations which break any preexisting symmetries of the system, demonstrating that discrete time-translation symmetry can be broken without another symmetry. We then generalize the field-theory description of the time-crystal phase [21] to the finite temperature dissipative phases obtained here.

Period-doubling in coupled parametric amplifiers.— We start by considering a coupled array of parametric oscillators with translational invariance in \mathcal{D} spatial dimensions. We choose to model such an array by a time-dependent Hamiltonian

$$H(t) = \sum_j \frac{1}{2} \dot{\phi}_j^2 + \frac{1}{2} \omega^2(t) \phi_j^2 + \frac{J}{2} \sum_{\hat{\mu}} (\phi_j - \phi_{j+\hat{\mu}})^2. \quad (1)$$

where $\omega(t+T) = \omega(t)$ is periodic in time and $\hat{\mu}$ iterates over each lattice vector. An individual periodically modulated oscillator can exhibit a parametric resonance [63, 64] featuring “amplified” and “squeezed” modes. As an illustration, we consider a piecewise-constant time dependence of the driving frequency $\omega(t) = \omega_1 \Theta(t/T - 1/2) + \omega_2 \Theta(-(t/T - 1/2))$, which is periodic in time with period T . Due to translation invariance, we can write the dynamics in terms of Bloch momentum modes $\psi_k = (\phi_k, \dot{\phi}_k)^T$. The Floquet time-evolution over period $[0, T]$ is given by a total transfer matrix M_k which equals the product of two 2×2 transfer matrices $M_k = M_{k,2} M_{k,1}$, each given by time-evolution of a harmonic oscillator with frequency $\omega_{j=1,2}$ and time $T/2$. Explicit forms are found in the Supplementary Material (SM). For an appropriate choice of model parameters, the transfer matrix M_k features amplified and squeezed modes, denoted ψ_k^A and ψ_k^S , with real eigenvalues λ_k and λ_k^{-1} . Without loss of generality, we assume $|\lambda_k| \geq 1$.

When the eigenvalue λ_k is less than -1 for some k , the parametric amplification can lead to an instability towards a period-doubled state where the parametrically amplified normal mode $\psi_k^A(t)$, as well as the corresponding displacement $\phi_k^A(t)$, switches sign between periods. Choosing the parameter J such that λ_k has a maximum at $k = 0$ leads to a spatially-uniform period-doubled extended state being dominant. However, the system is unstable to perturbations since $|\lambda_k| > 1$. We remedy

this by adding a damping to the equations of motion (a force proportional to $-\dot{\phi}$) such that the eigenvalues become $\lambda_k \rightarrow e^{-\Gamma T} \lambda_k$. Such a damping is naturally realized in Josephson junctions through a normal metal resistor or coupling to a transmission line, or in semiconductor laser systems from the finite quality factor of the cavity. At a critical damping $\Gamma_c = T^{-1} \log |\lambda_{k=0}|$, only the $k = 0$ period-doubled state persists. The steady state dynamics at this fine-tuned point features displacements $\phi_j(t)$ that are uniform in space and satisfy the period-doubling condition $\phi_j(T) = \phi_0(T) = -\phi_j(0)$ for all lattice sites j . Though this system shows period-doubled dynamics without any instability, it does not recover from applied perturbations and therefore does not satisfy the robustness criteria of a CDTC; the addition of weak noise and anharmonicity can stabilize this state into a true CDTC.

Perturbative nonlinearity and noise.— We perturb away from the fine-tuned point by setting the damping to $\Gamma = \Gamma_c - \epsilon(\nu/2T)$ where ν is a constant factor which we add for later convenience and $\epsilon \ll 1$. This change causes a small region around $k = 0$ to be unstable, shown in Fig. 1. Motivated by model A dynamics of a symmetry breaking system [51], we add a small nonlinear force

$$f_k(t) = \epsilon \sum_j e^{-ikj} \left[-g \phi_j(t)^3 + \frac{\nu}{2T} \dot{\phi}_j(t) + \eta_j(t) \right]. \quad (2)$$

which is proportional to ϵ to stabilize the amplification in this region. In this expression, the terms represent a restoring nonlinear force, the reduction in damping, and uncorrelated Gaussian noise with variance $\langle \eta_i(t) \eta_j(t') \rangle = 2D_m \delta_{ij} \delta(t - t')$ respectively. Since ϵ is small, the oscillatory micromotion is approximately exact while the slow dynamics is well approximated by discrete samples at times nT . This is analogous to the separation of dynamics in quantum Floquet systems [65]. Here g sets the positions of the fixed points generated by the nonlinear restoring force. While the nonlinearity is crucial for ensuring stability, the noise is also important to avoid the complexities of nonlinear many-body Hamiltonian dynamics, averting singularities by broadening transition probabilities [47, 48]

Applying the force $f_k(t)$, the evolution for ψ_k over a time-step $2nT$ is written as

$$\begin{aligned} \psi_k(2nT) &= (1 + \nu\epsilon/2)^{2n} M_k^{2n} \psi_k(0) \\ &+ \epsilon \int_0^{2nT} d\tau G_k(2nT, \tau) e_2 F_k[\{\psi_k\}, \tau] \\ &+ \epsilon \int_0^{2nT} d\tau G_k(2nT, \tau) e_2 \eta_k(\tau) \quad (3) \\ F_k[\{\psi_k\}, t] &\equiv -g \int dk_{1,2} \phi_{k_1}(t) \phi_{k_2}(t) \phi_{-k_1-k_2}(t). \end{aligned}$$

Here, the Greens function G_k generalizes the transfer matrix to continuous times ($G_k(nT, 0) = M_k^n$) and describes the fast dynamics of the parametric oscillators. The unit

vectors $e_2 = (0, 1)^T$ pick out the momentum component of the Greens function matrix.

Choosing n to be sufficiently large so that the squeezed eigenvalue of M_k^{2n} becomes comparable to ϵ for all momenta we observe that the total amplitude of the squeezed mode in $\psi_k(2nT)$ must be on the order of ϵ . The squeezed mode's effect on the amplified mode via the nonlinearity is then proportional to ϵ^2 and we can safely ignore its contribution to understand the steady state dynamics of the amplified mode, taking $\psi_k \simeq \psi_k^A$ and $\phi_k \simeq \phi_k^A$. Using this assumption, we can write the steady-state equation of motion over two periods as

$$\begin{aligned} \phi_k(2T) &= (1 + \nu\epsilon)\lambda_k^2\phi_k(0) + \epsilon\zeta_k \\ &- \epsilon g \int dk_{1,2} \xi_{k,k_1,k_2} \phi_{k_1}(0)\phi_{k_2}(0)\phi_{k-k_1-k_2}(0) \end{aligned} \quad (4)$$

to first order in ϵ . The coefficient ξ_{k,k_1,k_2} and the effective noise ζ_k encode the nonlinear effects and the stochastic process over two driving periods.

Scaling the momenta $k \rightarrow k\sqrt{\epsilon}$, which we can safely perform in the thermodynamic limit, allows us to expand the momentum-dependent amplification rate as

$$(1 + \nu\epsilon)\lambda_k^2 = (1 + \nu\epsilon) - \epsilon\gamma k^2 + O(\epsilon^2). \quad (5)$$

Furthermore, the coefficient for the nonlinear term and the noise strength both become k -independent up to leading order in ϵ , allowing us to replace ξ_{k,k_1,k_2} with $\xi \equiv \xi_{0,0,0}$ and assert that ζ_k has a constant variance. With these assumptions, focusing on the displacement component of ψ_k^A , we can approximate the discrete map in Eq. 4 as continuous dynamics by rescaling $T \rightarrow T\epsilon$. This yields a real-space Langevin equation

$$\dot{\phi}_i = -\frac{1}{2T} \left(\frac{\delta H}{\delta \phi_i} + \zeta_i \right) \quad (6)$$

with the Ginzburg-Landau (GL) Hamiltonian

$$H[\{\phi_i\}] = \sum_i -\frac{\nu}{2}\phi_i^2 + \frac{\gamma}{4}(\nabla\phi_i)^2 + \frac{g\xi}{4}\phi_i^4. \quad (7)$$

In this form, Eq. 6 is also known as a time-dependent Ginzburg-Landau equation. The variance of noise $\zeta_i(t)$ is $4T\epsilon D$, which includes a factor of $2T\epsilon$ from the conversion to a function of continuous time. (Explicit formulae for D and ξ are given in the SM.)

The Langevin equation relaxes the system towards the Boltzmann distribution associated with the GL Hamiltonian [60]

$$p[\{\phi_k\}] \sim e^{-H[\{\phi_k\}]/\epsilon D}. \quad (8)$$

This steady state distribution, for systems with dimension two or higher, shows spontaneous symmetry breaking of the $\phi \rightarrow -\phi$ Ising symmetry when the parameter ν in Eq. 7 is greater than a critical value ν_c . In this

case, the dynamics on the even time steps $2nT$ breaks ergodicity [60] into configurations

$$\langle \phi_i(2nT) \rangle = \text{constant}, \quad (9)$$

breaking the Ising symmetry of the Hamiltonian H . (At odd time steps, this constant has the opposite sign since the eigenvalue λ_k is less than one.) Using known data on the GL phase transition on a 2D lattice [56], we calculate the phase boundary, delineated by $\nu = \nu_c$, in terms of microscopic parameters, shown in the inset of Fig. 1. This transition can be extended to one dimension by introducing long-range interactions $O(1/r^\alpha)$ for $1 < \alpha < 2$ [66]. We therefore expect a CDTC phase transition at a critical noise strength when $1 < \alpha < 2$, which is consistent with the result cellular automata result from 67.

Robustness.— The Ising symmetry $\phi \mapsto -\phi$ played a crucial role in the GL treatment of symmetry breaking described in the previous section. However as a matter of principle, the time-crystal phase should be robust to perturbations that break this symmetry [68]. To demonstrate that the time-crystal phase is indeed robust, we describe the time crystal phase in this system without any reference to an Ising symmetry through an order parameter

$$O = \bar{\phi}(2nT) - \bar{\phi}((2n-1)T) \quad (10)$$

whose expectation value is a measure of time translation symmetry breaking and $\bar{\phi} = L^{-d} \sum_i \phi_i$ is the average magnetization over the system. This time-crystal order parameter is non-zero in the Ising symmetric GL system described by Eq. 9 together with the period doubling condition $\phi_i(2nT) \simeq -\phi_i((2n-1)T)$.

We verify this robustness using a Markov chain Monte Carlo simulation of overdamped dynamics by replacing the Langevin dynamics in Eq. 6 by Glauber dynamics [69] on the GL Hamiltonian in Eq. 7 together with a symmetry breaking term $\sum_i d\phi_i^3$. This implements a discrete dynamics similar to Eq. 4 rather than the continuous time limit in Eq. 6. A similar approach was taken in Ref. 70. While the Glauber dynamics, in general, differs from the oscillator evolution (i.e. Eq. 3), it reproduces the GL stationary distribution obtained from Eq. 4 in the limit of small ϵ so that the dynamics is easy to calibrate. We then model the period doubling property of each oscillator as a global flip $\phi \mapsto -\phi$ at each time step T . We measure the time crystal order parameter O on a 2D lattice and find a phase transition that persists for finite d in Fig. 2, though with a different critical point. Due to the asymmetry, the time-averaged magnetization $\langle \bar{\phi} \rangle$ deviates from the symmetric point at $\bar{\phi} = 0$, indicating that the Ising symmetry is truly broken. This behavior indicates that the periodic drive creates an emergent Ising symmetry which is analogous to that of the π -spin glass system in the quantum case [68, 71]. The phase transition remains robust up until $d \approx 1$, where the sys-

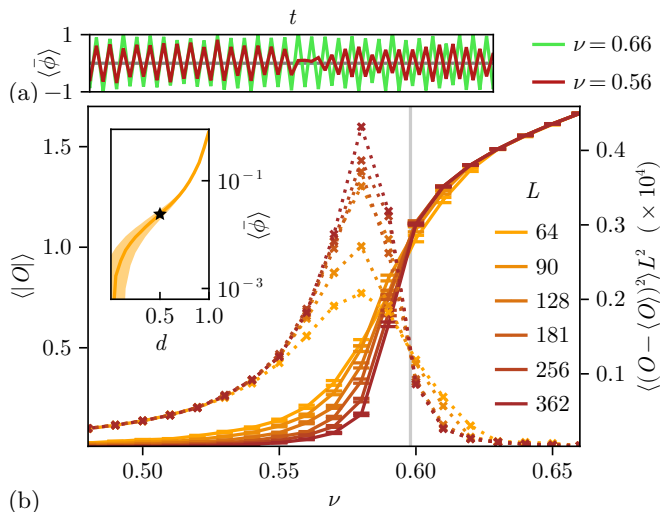


FIG. 2. (a) Demonstration of phase-slip in the symmetric phase (red) compared with broken phase (green); (b) Order parameter O (Eq. 10, solid lines) and susceptibility (dotted lines) in the 2D asymmetric ϕ^4 model demonstrating a second-order phase transition in the quadratic coefficient at $\nu_c \approx 0.598$ (grey line) with an asymmetry of $d = 0.5$, compared to $\nu_c = 0.72112$ for the symmetric model [56]. The inset shows time-averaged magnetization $\langle \bar{\phi} \rangle$ as a function of asymmetry strength, with a black star at $d = 0.5$ denoting the value for the main plot. $\gamma = 4$, $g\xi = 0.5$, $\epsilon D = 2$.

tem no longer features time-crystalline behavior. More details are found in the Supplementary Material.

To further understand these results, we formally define the coarse-grained Markov chain dynamics at the time steps $t = nT$ as

$$\psi_i((n+1)T) = Q_i[\{\psi_j(nT)\}] \quad (11)$$

where Q_i is a random functional of the displacement and momentum configurations $\{\psi_j\}$. Since Q_i is local, the process is equivalent to a local Markov process or a PCA. This dynamical map generates a Markov process with a transition probability

$$\mathcal{L}[\{\psi'_i|\{\psi_j\}] = \left\langle \prod_i \delta(\psi'_i - Q_i[\{\psi_j\}]) \right\rangle. \quad (12)$$

that evolves the probability distribution between times nT and $(n+1)T$. Here, δ is the Dirac delta function. For simplicity, we will represent \mathcal{L} as a linear operator on the space of probability distribution vectors $p[\{\psi_k\}]$ through the relation

$$(\mathcal{L}p)[\{\psi_k\}] \equiv \int D\psi'_{k'} L[\{\psi_k|\{\psi'_{k'}\}] p[\{\psi'_{k'}\}]. \quad (13)$$

The above equation can also be viewed as an evolution equation for a quantum system with a Markovian dissipation (e.g. via a Lindblad master equation [33]) if the probability $p[\{\psi_k\}] \rightarrow p[\{\psi_{-k}^*, \psi_k\}]$ is a Wigner representation of the quantum density matrix. Note that in

the quantum case, it is more convenient to change the fundamental variables to $\psi_k \simeq \phi_k + i\dot{\phi}_k$ which would represent the oscillator position and momenta in a coherent state representation. The linear operator \mathcal{L} is the time-evolution of the density matrix over T , which is an exponential of the Lindblad superoperator. The classical equations of motion Eq. 3 can be obtained from the truncated Wigner approximation [72] of the quantum evolution in the large occupation/weak interaction limit of the oscillator modes. We will allow $p[\{\psi_k\}]$ to be a density matrix in the rest of the work.

Since the transition probabilities depend only on the instantaneous state of the system, the dynamics form a Markov chain that is finite¹ and ergodic and therefore admits a stationary probability distribution $p^*[\{\psi_i\}]$ (the asterisk here denotes stationarity, not complex conjugation). In the quantum case, p^* is the stationary solution of the quantum master equation. Taking the logarithm of this distribution gives an effective Hamiltonian

$$H[\{\psi_i\}] \propto -\log p^*[\{\psi_i\}]. \quad (14)$$

This is similar to the effective Hamiltonian of pre-thermal quantum systems [21]. To understand magnetic phases, it is more insightful to consider the probability distribution of the magnetization $\bar{\phi}$ written as:

$$P(M) = \langle \delta(M - \bar{\phi}) \rangle_{p^*}. \quad (15)$$

In a system without continuous symmetries, for short range correlated phases, the central limit theorem suppresses the variance of the mean magnetization. Systems that are not critical are typically short range correlated except when the system breaks symmetry spontaneously and the system separates into phases with different mean magnetizations [60]. We thus expect $P(M)$ to be sharply peaked in the thermodynamic limit. Specifically, $P(M)$ approaches a weighted sum of Dirac delta functions in the thermodynamic limit. This is analogous to coexistence in equilibrium spontaneous symmetry breaking.

We now pick one delta peak at $M = M_1$ and choose a neighborhood \mathcal{N} in the space of magnetizations such that M_1 is the only peak in \mathcal{N} . We then define the conditional probability distribution

$$p_{\mathcal{N}}^*[\{\psi_i\}] \equiv p^*[\{\psi_i\} | \bar{\phi} \in \mathcal{N}] \quad (16)$$

which does not exhibit coexistence or long range order. The corresponding density matrix in the quantum case, which would be defined by applying a projector $\mathcal{P}_{\bar{\phi} \in \mathcal{N}}$, is analogous to the symmetry breaking density matrix in the prethermal case [21]. The magnetization after one time step is then

$$M_2 = \langle \phi_i \rangle_{\mathcal{L}p_{\mathcal{N}}^*}. \quad (17)$$

¹ Though we are ultimately interested in the thermodynamic limit, any given system size is finite in the mathematical sense.

If $M_2 \neq M_1$, then this map defines a distinct delta peak in $P(M)$ around M_2 . One can check that in this case, if p_N^* is stationary under the Markov chain \mathcal{L}^2 , then \mathcal{L} defines a period-2 discrete time crystal. Due to the peaked structure of p^* , we can relax these conditions to

$$\langle \bar{\phi} \rangle_{\mathcal{L}p_N^*} \notin \mathcal{N}, \quad \langle \bar{\phi} \rangle_{\mathcal{L}^2 p_N^*} \in \mathcal{N}. \quad (18)$$

While it is clear that these conditions lead to DTC behavior in infinite systems, we claim that satisfactory systems for any size N must have a diverging autocorrelation time as $N \rightarrow \infty$. In a large but finite-sized system, we can soften the definition of \mathcal{N} to including only one maximum of $P(M)$. For example, \mathcal{N} can be chosen to be the region around M_1 over which $P(M)$ is concave, which we expect roughly maximizes the likelihood that the conditions correctly identify CDTC behavior. Since the magnetization is intensive, the positions of the peaks are independent of system size and \mathcal{N} encompasses only one peak as $N \rightarrow \infty$, satisfying the aforementioned condition. We note that this argument may not extend to period- n symmetry breaking for $n > 2$ [73].

In a finite-sized system, a phase slip in the CDTC order O occurs if the magnetization at any given time step falls inside the neighborhood \mathcal{N} after one time-step or outside after two time-steps. Assuming Eq. 18, such a phase slip may have a nonzero probability due to the variance of $\bar{\phi}$. The probability of a phase slip is related to the variance of $\bar{\phi}$ under $\mathcal{L}^n p_N^*$ for $n = 0, 1$ and 2 , which decays exponentially in L^{d-1} (as opposed to L^d , due to domain walls).

Incidentally, the temperature of the classical system considered here needs to be low (i.e. $o(\epsilon)$) since the microscopic noise power scales as ϵ (since $\epsilon D_m \sim o(1)$ in Eq. 8) while the microscopic damping scales as unity. These considerations should be relevant to evidence for dissipative quantum time crystals in recent experiments [36].

Discussion.— We have considered the possibility of a CDTC state in a coupled array of period-doubling parametric amplifiers and explained how our results can be robust in a more general context of PCAs. Since parametric amplifiers occur in many driven, weakly dissipative nonlinear systems such as Josephson junctions [59, 74, 75], nonlinear optics [76] and nonlinear electronic circuit elements [77], we are optimistic that this analysis motivates experimental studies of CDTC symmetry breaking in more systems.

Using a course-grained mapping to Glauber dynamics that was solved numerically as well as a field-theoretic [21] argument, we have shown that the CDTC phase obtained is absolutely stable [23] and robust to Ising symmetry breaking and other perturbations. The field-theoretic argument implies conditions for identifying a CDTC that apply to translation-invariant systems without continuous symmetries and with a spatially self-averaging order-parameter. Additionally, the classical system discussed can be viewed as the semiclassical limit

of the corresponding quantum system in the so-called truncated Wigner approximation [72]. The robustness argument using the field-theoretical formalism extends to quantum corrections. The central difference between our analysis and the one in closed quantum systems [21], where the CDTC phase is prethermal, appears to be the presence of dissipation instead of disorder. The presence of disorder can complicate the identification of an order parameter [21]. A better understanding of CDTC systems with disorder and dissipation is an interesting future direction.

We thank Francisco Machado for alerting us to the emergent Ising symmetry in time crystals. We also thank Sankar Das Sarma, DinhDuy Vu, Tom Iadecola and Paul Goldbart for valuable comments on the work. S.Y.T. thanks the Joint Quantum Institute at the University of Maryland for support through a JQI fellowship. J.S. acknowledges support from the Joint Quantum Institute as well as valuable discussions hosted at the Aspen Center for Physics, which is supported by National Science Foundation grant PHY-2210452. This work is also supported by the Laboratory for Physical Sciences through its continuous support of the Condensed Matter Theory Center at the University of Maryland.

-
- [1] F. Wilczek, Quantum time crystals, *Physical Review Letters* **109**, 160401 (2012).
 - [2] T. Li, Z.-X. Gong, Z.-Q. Yin, H. T. Quan, X. Yin, P. Zhang, L.-M. Duan, and X. Zhang, Space-time crystals of trapped ions, *Physical Review Letters* **109**, 163001 (2012).
 - [3] D. V. Else, B. Bauer, and C. Nayak, Floquet time crystals, *Physical Review Letters* **117**, 090402 (2016).
 - [4] P. Bruno, Impossibility of spontaneously rotating time crystals: A no-go theorem, *Physical Review Letters* **111**, 070402 (2013).
 - [5] H. Watanabe and M. Oshikawa, Absence of quantum time crystals, *Physical Review Letters* **114**, 251603 (2015).
 - [6] K. Sacha, Modeling spontaneous breaking of time-translation symmetry, *Physical Review A* **91**, 033617 (2015).
 - [7] D. V. Else, C. Monroe, C. Nayak, and N. Y. Yao, Discrete time crystals, *Annual Review of Condensed Matter Physics* **11**, 467 (2020).
 - [8] V. Khemani, A. Lazarides, R. Moessner, and S. L. Sondhi, Phase structure of driven quantum systems, *Physical Review Letters* **116**, 250401 (2016).
 - [9] R. Moessner and S. L. Sondhi, Equilibration and order in quantum floquet matter, *Nature Physics* **13**, 424–428 (2017).
 - [10] N. Y. Yao, A. C. Potter, I.-D. Potirniche, and A. Vishwanath, Discrete time crystals: Rigidity, criticality, and realizations, *Physical Review Letters* **118**, 030401 (2017).
 - [11] F. Machado, Q. Zhuang, N. Y. Yao, and M. P. Zaletel, Absolutely stable time crystals at finite temperature, *Physical Review Letters* **131**, 10.1103/phys-

- revlett.131.180402 (2023).
- [12] L. D'Alessio and M. Rigol, Long-time behavior of isolated periodically driven interacting lattice systems, *Physical Review X* **4**, 041048 (2014).
- [13] A. Lazarides, A. Das, and R. Moessner, Equilibrium states of generic quantum systems subject to periodic driving, *Physical Review E* **90**, 012110 (2014).
- [14] P. Ponte, A. Chandran, Z. Papić, and D. A. Abanin, Periodically driven ergodic and many-body localized quantum systems, *Annals of Physics* **353**, 196–204 (2015).
- [15] A. Lazarides, A. Das, and R. Moessner, Fate of many-body localization under periodic driving, *Physical Review Letters* **115**, 030402 (2015).
- [16] P. Ponte, Z. Papić, F. Huveneers, and D. A. Abanin, Many-body localization in periodically driven systems, *Physical Review Letters* **114**, 140401 (2015).
- [17] A. Lazarides and R. Moessner, Fate of a discrete time crystal in an open system, *Physical Review B* **95**, 195135 (2017).
- [18] A. Pizzi, D. Malz, G. De Tomasi, J. Knolle, and A. Nunnenkamp, Time crystallinity and finite-size effects in clean floquet systems, *Physical Review B* **102**, 214207 (2020).
- [19] W. Hodson and C. Jarzynski, Energy diffusion and absorption in chaotic systems with rapid periodic driving, *Physical Review Research* **3**, 013219 (2021).
- [20] D. Abanin, W. De Roeck, W. W. Ho, and F. Huveneers, A rigorous theory of many-body prethermalization for periodically driven and closed quantum systems, *Communications in Mathematical Physics* **354**, 809–827 (2017).
- [21] D. V. Else, B. Bauer, and C. Nayak, Prethermal phases of matter protected by time-translation symmetry, *Physical Review X* **7**, 011026 (2017).
- [22] T.-S. Zeng and D. N. Sheng, Prethermal time crystals in a one-dimensional periodically driven floquet system, *Physical Review B* **96**, 094202 (2017).
- [23] F. Machado, D. V. Else, G. D. Kahanamoku-Meyer, C. Nayak, and N. Y. Yao, Long-range prethermal phases of nonequilibrium matter, *Physical Review X* **10**, 011043 (2020).
- [24] M. Natsheh, A. Gambassi, and A. Mitra, Critical properties of the prethermal floquet time crystal, *Physical Review B* **103**, 224311 (2021).
- [25] A. Pizzi, A. Nunnenkamp, and J. Knolle, Classical prethermal phases of matter, *Physical Review Letters* **127**, 140602 (2021).
- [26] A. Pizzi, A. Nunnenkamp, and J. Knolle, Classical approaches to prethermal discrete time crystals in one, two, and three dimensions, *Physical Review B* **104**, 094308 (2021).
- [27] B. Ye, F. Machado, and N. Y. Yao, Floquet phases of matter via classical prethermalization, *Physical Review Letters* **127**, 140603 (2021).
- [28] R. Citro, E. G. Dalla Torre, L. D'Alessio, A. Polkovnikov, M. Babadi, T. Oka, and E. Demler, Dynamical stability of a many-body Kapitza pendulum, *Annals of Physics* **360**, 694–710 (2015).
- [29] N. Y. Yao, C. Nayak, L. Balents, and M. P. Zaletel, Classical discrete time crystals, *Nature Physics* **16**, 438–447 (2020).
- [30] R. Khasseh, R. Fazio, S. Ruffo, and A. Russomanno, Many-body synchronization in a classical hamiltonian system, *Physical Review Letters* **123**, 184301 (2019).
- [31] H. Keßler, J. G. Cosme, C. Georges, L. Mathey, and A. Hemmerich, From a continuous to a discrete time crystal in a dissipative atom-cavity system, *New Journal of Physics* **22**, 085002 (2020).
- [32] D. D. Vu and S. Das Sarma, Dissipative prethermal discrete time crystal, *Physical Review Letters* **130**, 130401 (2023).
- [33] G. Passarelli, P. Lucignano, R. Fazio, and A. Russomanno, Dissipative time crystals with long-range lindbladians, *Physical Review B* **106**, 224308 (2022).
- [34] A. Lazarides, S. Roy, F. Piazza, and R. Moessner, Time crystallinity in dissipative floquet systems, *Physical Review Research* **2**, 022002(R) (2020).
- [35] X. Nie and W. Zheng, Mode softening in time-crystalline transitions of open quantum systems, *Physical Review A* **107**, 033311 (2023).
- [36] H. Kessler, P. Kongkhambut, C. Georges, L. Mathey, J. G. Cosme, and A. Hemmerich, Observation of a dissipative time crystal, *Physical Review Letters* **127**, 043602 (2021).
- [37] S. Choi, J. Choi, R. Landig, G. Kucsko, H. Zhou, J. Isoya, F. Jelezko, S. Onoda, H. Sumiya, V. Khemani, C. von Keyserlingk, N. Y. Yao, E. Demler, and M. D. Lukin, Observation of discrete time-crystalline order in a disordered dipolar many-body system, *Nature* **543**, 221–225 (2017).
- [38] J. Zhang, P. W. Hess, A. Kyprianidis, P. Becker, A. Lee, J. Smith, G. Pagano, I.-D. Potirniche, A. C. Potter, A. Vishwanath, N. Y. Yao, and C. Monroe, Observation of a discrete time crystal, *Nature* **543**, 217–220 (2017).
- [39] S. Pal, N. Nishad, T. S. Mahesh, and G. J. Sreejith, Temporal order in periodically driven spins in star-shaped clusters, *Physical Review Letters* **120**, 180602 (2018).
- [40] J. Rovny, R. L. Blum, and S. E. Barrett, Observation of discrete-time-crystal signatures in an ordered dipolar many-body system, *Physical Review Letters* **120**, 180603 (2018).
- [41] M. Ippoliti, K. Kechedzhi, R. Moessner, S. L. Sondhi, and V. Khemani, Many-body physics in the nisq era: Quantum programming a discrete time crystal, *PRX Quantum* **2**, 030346 (2021).
- [42] X. Mi, M. Ippoliti, C. Quintana, A. Greene, Z. Chen, J. Gross, F. Arute, K. Arya, J. Atalaya, R. Babush, J. C. Bardin, J. Basso, A. Bengtsson, A. Bilmes, A. Bourassa, *et al.*, Time-crystalline eigenstate order on a quantum processor, *Nature* **601**, 531–536 (2021).
- [43] P. Frey and S. Rachel, Realization of a discrete time crystal on 57 qubits of a quantum computer, *Science Advances* **8**, eabm7652 (2022).
- [44] A. Kyprianidis, F. Machado, W. Morong, P. Becker, K. S. Collins, D. V. Else, L. Feng, P. W. Hess, C. Nayak, G. Pagano, N. Y. Yao, and C. Monroe, Observation of a prethermal discrete time crystal, *Science* **372**, 1192–1196 (2021).
- [45] W. Bearez, O. Janes, A. Akkiraju, A. Pillai, A. Oddo, P. Reshetikhin, E. Druga, M. McAllister, M. Elo, B. Gilbert, D. Suter, and A. Ajoy, Floquet prethermalization with lifetime exceeding 90 s in a bulk hyperpolarized solid, *Physical Review Letters* **127**, 170603 (2021).
- [46] W. Bearez, C. Fleckenstein, A. Pillai, E. de Leon Sanchez, A. Akkiraju, J. Diaz Alcala, S. Conti, P. Reshetikhin, E. Druga, M. Bukov, and A. Ajoy, Critical prethermal discrete time crystal created by two-frequency driving, *Nature Physics* **19**,

- 407–413 (2023).
- [47] B. Van Der Pol and J. Van Der Mark, Frequency demultiplication, *Nature* **120**, 363–364 (1927).
- [48] S. H. Strogatz, *Nonlinear dynamics and chaos with student solutions manual: With applications to physics, biology, chemistry, and engineering* (CRC press, 2018).
- [49] S. E. Brown, G. Mozurkewich, and G. Grüner, Harmonic and subharmonic shapiro steps in orthorhombic tas3, *Solid state communications* **54**, 23 (1985).
- [50] W. Yu, E. B. Harris, S. E. Hebboul, J. C. Garland, and D. Stroud, Fractional shapiro steps in ladder josephson arrays, *Physical Review B* **45**, 12624 (1992).
- [51] P. C. Hohenberg and B. I. Halperin, Theory of dynamic critical phenomena, *Reviews of Modern Physics* **49**, 435 (1977).
- [52] T. Kontorova and J. Frenkel, On the theory of plastic deformation and twinning. II., *Zh. Eksp. Teor. Fiz.* **8**, 1340 (1938).
- [53] A. L. Toom, Nonergodic multidimensional system of automata, *Problemy Peredachi Informatsii* **10**, 70 (1974).
- [54] P. Gács, Reliable cellular automata with self-organization, *Journal of Statistical Physics* **103**, 45 (2001).
- [55] L. F. Gray, *Journal of Statistical Physics* **103**, 1–44 (2001).
- [56] D. Schaich and W. Loinaz, Improved lattice measurement of the critical coupling in ϕ^4 theory, *Physical Review D* **79**, 056008 (2009).
- [57] T. B. Simpson, J. M. Liu, A. Gavrielides, V. Kovanis, and P. M. Alsing, Period-doubling cascades and chaos in a semiconductor laser with optical injection, *Physical Review A* **51**, 4181 (1995).
- [58] A. Sarkar, Anurag, R. Singh, A. A. Makki, J. A. Mondal, A. K. Rathi, R. J. T. Nicholl, S. Chakraborty, K. I. Bolotin, and S. Ghosh, Observation of tunable discrete time crystalline phases (2023).
- [59] R. Vijay, M. H. Devoret, and I. Siddiqi, Invited Review Article: The Josephson bifurcation amplifier, *Review of Scientific Instruments* **80**, 111101 (2009), <https://pubs.aip.org/aip/rsi/article-pdf/doi/10.1063/1.3224703/16086135/111101.1.online.pdf>.
- [60] N. Goldenfeld, *Lectures on phase transitions and the renormalization group* (CRC Press, 2018).
- [61] R. B. Griffiths, C.-Y. Weng, and J. S. Langer, Relaxation times for metastable states in the mean-field model of a ferromagnet, *Physical Review* **149**, 301 (1966).
- [62] H. Tomita and S. Miyashita, Statistical properties of the relaxation processes of metastable states in the kinetic ising model, *Physical Review B* **46**, 8886 (1992).
- [63] L. Landau and E. Lifshitz, *Mechanics Third Edition: Volume 1 of Course of Theoretical Physics* (Elsevier, 1976) Chap. 27.
- [64] G. Floquet, Sur les équations différentielles linéaires à coefficients périodiques, *Annales scientifiques de l'École Normale Supérieure* **12**, 47 (1883).
- [65] A. Eckardt and E. Anisimovas, High-frequency approximation for periodically driven quantum systems from a floquet-space perspective, *New Journal of Physics* **17**, 093039 (2015).
- [66] F. J. Dyson, Existence of a phase-transition in a one-dimensional ising ferromagnet, *Communications in Mathematical Physics* **12**, 91–107 (1969).
- [67] A. Pizzi, A. Nunnenkamp, and J. Knolle, Bistability and time crystals in long-ranged directed percolation, *Nature Communications* **12**, 1061 (2021).
- [68] C. W. von Keyserlingk, V. Khemani, and S. L. Sondhi, Absolute stability and spatiotemporal long-range order in floquet systems, *Physical Review B* **94**, 085112 (2016).
- [69] R. J. Glauber, Time-dependent statistics of the ising model, *Journal of Mathematical Physics* **4**, 294–307 (1963).
- [70] F. M. Gambetta, F. Carollo, A. Lazarides, I. Lesanovsky, and J. P. Garrahan, Classical stochastic discrete time crystals, *Physical Review E* **100**, 060105 (2019).
- [71] V. Khemani, C. W. von Keyserlingk, and S. L. Sondhi, Defining time crystals via representation theory, *Physical Review B* **96**, 115127 (2017).
- [72] A. Polkovnikov, Quantum corrections to the dynamics of interacting bosons: Beyond the truncated wigner approximation, *Physical Review A* **68**, 053604 (2003).
- [73] C. H. Bennett, G. Grinstein, Y. He, C. Jayaprakash, and D. Mukamel, Stability of temporally periodic states of classical many-body systems, *Physical Review A* **41**, 1932 (1990).
- [74] O. Yaakobi, L. Friedland, C. Macklin, and I. Siddiqi, Parametric amplification in josephson junction embedded transmission lines, *Physical Review B* **87**, 144301 (2013).
- [75] A. Russomanno, Spatiotemporally ordered patterns in a chain of coupled dissipative kicked rotors, *Physical Review B* **108**, 094305 (2023).
- [76] E. Galiffi, R. Tirole, S. Yin, H. Li, S. Vezzoli, P. A. Huidobro, M. G. Silveirinha, R. Sapienza, A. Alù, and J. Pendry, Photonics of time-varying media, *Advanced Photonics* **4**, 014002 (2022).
- [77] S. Ranganathan and Y. Tsvividis, Discrete-time parametric amplification based on a three-terminal mos varactor: Analysis and experimental results, *IEEE Journal of Solid-State Circuits* **38**, 2087 (2003).

Supplementary Material for “Theory for dissipative time crystals in coupled parametric oscillators”

DETAILS OF PARAMETRIC AMPLIFICATION

Consider the Hamiltonian

$$H(t) = \sum_j \frac{1}{2} \dot{\phi}_j^2 + \frac{1}{2} \omega^2(t) \phi_j^2 + \frac{J}{2} (\phi_j - \phi_{j+1})^2. \quad (1)$$

Spatial translation invariance allows us to decouple the oscillators into independent Bloch momentum modes, represented as vectors in phase space $\psi_k = (\phi_k, \dot{\phi}_k)^T$. Allowing for the possibility of a damping Γ to each oscillator, the equation of motion of the Fourier component $\phi_k(t)$ is written as $\ddot{\phi}_k = -[\omega_0^2(t) + 2J \sin^2(k/2)] \phi_k - \Gamma \dot{\phi}_k$. We factor out this damping by defining $\tilde{\phi}_k \equiv e^{\Gamma t/2} \phi_k$ such that the damping term can be eliminated from the equation of motion

$$\ddot{\tilde{\phi}}_k = -\Omega_k^2(t) \tilde{\phi}_k, \quad (2)$$

where

$$\Omega_k^2(t) \equiv \omega_0^2(t) + 2J \sin^2(k/2) - (\Gamma/2)^2. \quad (3)$$

We can also relate the two-component phase-space vector ψ_k to its damped counterpart $\tilde{\psi}_k$ using the transformation $\tilde{\psi}_k = P_\Gamma e^{\Gamma t/2} \psi_k$ where $P_\Gamma \equiv \begin{pmatrix} 1 & 0 \\ \Gamma/2 & 1 \end{pmatrix}$.

To understand the dynamics using Floquet analysis [1], we describe the motion over one driving period with the transfer matrix M_k such that $\psi_k(T) = M_k \psi_k(0)$, or $\tilde{\psi}_k(T) = \tilde{M}_k \tilde{\psi}_k(0)$ for the damped phase space vector. In the case where $\omega_0(t)$ is time-independent, M_k is effectively unitary (i.e. with eigenvalues of unit magnitude) and the modes preserve their amplitude in a way to conserve the energy. More interesting behavior can be obtained when $\omega_0(t)$ is parametrically time-dependent at a driving frequency around half of the natural frequency. Such a driven oscillator leads to parametric resonance [2] featuring “amplified” and “squeezed” modes.

For the purpose of illustration, we consider a general piecewise-constant time dependence of the driving frequency

$$\omega_0(t) = \begin{cases} \omega_1 & \{ \frac{t}{T} \} < \frac{1}{2} \\ \omega_2 & \{ \frac{t}{T} \} \geq \frac{1}{2} \end{cases}, \quad (4)$$

where curly brackets denote the fractional part. Since the corresponding frequency $\Omega_k(t)$ is also piecewise constant in time, we abbreviate its values as $\Omega_{k,j}$ where $j = 1, 2$ following Eq. 4. We then calculate the total transfer matrix \tilde{M}_k as the product of two transfer matrices $\tilde{M}_k = \tilde{M}_{k,2}(T/2) \tilde{M}_{k,1}(T/2)$ where $\tilde{M}_{k,j}$ is the transfer matrix over the time-independent regions of the drive:

$$\tilde{M}_{k,j}(t) = \exp \left[\begin{pmatrix} 0 & 1 \\ -\Omega_{k,j}^2 & 0 \end{pmatrix} t \right]. \quad (5)$$

Since \tilde{M}_k has determinant 1, its trace is $\text{tr} \tilde{M}_k = \lambda_k + \lambda_k^{-1}$ where λ_k and λ_k^{-1} are the eigenvalues of \tilde{M}_k . Assuming without loss of generality that $|\lambda_k| \geq 1$, the parametric oscillator at wave-vector k demonstrates amplifying behavior when $|\lambda_k| > 1$. Since \tilde{M}_k is real, and $|\lambda_k| \neq |\lambda_k^{-1}|$, the eigenvalue λ_k must be real. The driven oscillator then displays a parametric resonance when $|\text{tr} \tilde{M}_k| > 2$.

The parametric amplification can lead to an instability towards a period-doubled state when $\text{tr} \tilde{M}_k < -2$ since in this case, the eigenvalues λ_k are negative real numbers. As a result the parametrically amplified normal mode $\psi_k^A(t)$, as well as the corresponding displacement $\phi_k^A(t)$, switches sign between periods:

$$\begin{aligned} \psi_k^A(T) &= P_\Gamma^{-1} e^{-\Gamma T/2} \tilde{M}_k P_\Gamma \psi_k^A(0) \\ &= \lambda_k e^{-\Gamma T/2} \psi_k^A(0) \\ &= -|\lambda_k| e^{-\Gamma T/2} \psi_k^A(0). \end{aligned} \quad (6)$$

Such a period-doubling parametric amplification at wave-vector k occurs when the parameters $\Omega_{k,j}$ satisfy

$$\delta\Omega_k^2 \cos \delta\Omega_k - \bar{\Omega}_k^2 \cos \bar{\Omega}_k > \Omega_{k,1}\Omega_{k,2} \quad (7)$$

where $\bar{\Omega}_k = (\Omega_{k,1} + \Omega_{k,2})/2$ and $\delta\Omega_k = (\Omega_{k,1} - \Omega_{k,2})/2$, scaling the driving period to $T = 1$.

As shown in Appendix , our choice of $\Omega_{k,j}$ resulting from Eq. 3 and Eq. 4 maximizes the period-doubling parametric amplification eigenvalue $|\lambda_k e^{-\Gamma T/2}|$ at $k = 0$. Thus, if we choose a critical damping Γ_c such that $\Gamma_c T/2 = \log \lambda_{k=0} - \epsilon$, where $\epsilon > 0$ is an infinitesimally small parameter, the coupled system of parametric oscillators described by Eq. 1 together with damping shows period-doubling amplification at $k = 0$. Physically, this means that each oscillator $\phi_j(t)$ satisfies the period-doubling condition $\phi_j(T) = -\phi_j(0)$ for all lattice sites j . This state of the coupled parametric oscillator, starting from any initial displacement, becomes a steady state of all oscillators where the $k = 0$ parametric amplified state takes over i.e.

$$\phi_j(nT) \rightarrow (-1)^n (1 + \epsilon)^n \phi(0), \quad (8)$$

as $n \rightarrow \infty$ where $\phi(0)$ is an initial amplitude, which is slowly amplified for $\epsilon > 0$. Fig. ?? shows the range of wave-vectors k over which such amplification occurs as a function of average natural frequency for specific optimal parameters (detailed in Appendix). In addition to the amplified region, the figure shows a unbifurcated region where the modes are related by complex conjugation and show periodic dynamics at a frequency near the average natural frequency. These modes are attenuated at the rate of the externally imposed damping, without which the dynamics would be equivalent to a simple harmonic oscillator. Since the results in the figure are for a system with a finite amount of damping, the figure also supports an attenuated region in addition to the amplified and unbifurcated region. This region is characterized by dynamics that is attenuated at a rate slower than the externally imposed damping. In fact, in the absence of such damping, the amplified region would expand to include all of the attenuated range.

This state in the fine-tuned limit of $\epsilon = 0$ reaches an exact period-doubled steady state, exhibiting subharmonic entrainment. However, this does not satisfy the robustness criteria of a CDTC since it is sensitive to changes in Γ or other parameters of the system. Furthermore, the dynamics of this state is in some sense critical; i.e. it takes a divergent amount of time for the system to approach the period-doubled state. However, as we will show in the next section, the addition of weak noise and anharmonicity can stabilize this state into a CDTC.

To achieve a $k = 0$ period-doubled regime with amplified and squeezed modes, we explicitly write the trace of $\tilde{M}_{k=0}$ as

$$\text{tr } \tilde{M}_{k=0} = 2 \cos(\theta_1 + \theta_2) - \frac{(\theta_1 - \theta_2)^2 \sin \theta_1 \sin \theta_2}{\theta_1 \theta_2}$$

where $\theta_i = \Omega_{k=0,i} T/2$. Now we can set $\theta_1 + \theta_2 = \pi$ to make the first term -2 . The trace then becomes

$$\text{tr } \tilde{M}_{k=0} = -2 - \frac{4\varphi^2 \cos^2 \varphi}{\frac{\pi^2}{4} - \varphi^2}$$

where $\varphi \equiv (\theta_2 - \theta_1)/2$. The minimum value of this trace, corresponding to the greatest amount of amplification, is the solution to a transcendental equation $\varphi - \frac{4}{\varphi^3}/\pi^2 = \cot \varphi$ in the range $0 < \varphi < \pi/2$. Numerically, this value is 0.332π which gives a minimum trace of ≈ -2.8 . We use this value throughout the paper.

EXPLICIT FORMULAE FOR GINZBURG-LANDAU PARAMETERS

We give the explicit formulae for the parameters of the Ginzburg-Landau Hamiltonian

$$H[\{\phi_i\}] = \sum_i -\frac{\nu}{2} \phi_i^2 + \frac{\gamma}{4} (\nabla \phi_i)^2 + \frac{g\xi}{4} \phi_i^4 \quad (9)$$

found in the main text:

$$\begin{aligned} \xi_{k,k_1,k_2} &= \int_0^{2T} d\tau A_k(2T - \tau) B_{k_1}(\tau) B_{k_2}(\tau) B_{k-k_1-k_2}(\tau) \\ \zeta_k &= \int_0^{2T} d\tau A_k(2T - \tau) \eta_k(\tau). \end{aligned} \quad (10)$$

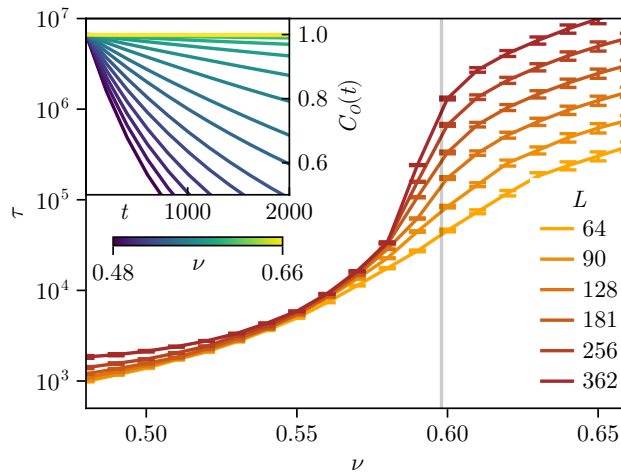


FIG. 1. Autocorrelation time τ as a function of GL parameter ν , measured by fitting the autocorrelator $C_O(t)$ of the order parameter O (shown in the inset) to an exponential. See main text Fig. 2 for simulation details.

where

$$A_k(t) = [V_k^{-1}G_k(t)]_{12}$$

$$B_k(t) = [G_k(t)V_k]_{11}.$$

Here V_k is the matrix with the eigenvectors of $G_k(T)$ as columns (amplified first).

After scaling $k \rightarrow k\sqrt{\epsilon}$, the variance of ζ_k becomes

$$4T\epsilon D = \int dt' \langle \zeta_k(t)\zeta_k(t') \rangle \quad (11)$$

$$= (2T\epsilon) \langle \zeta_k^2 \rangle \quad (12)$$

$$= 4T\epsilon D_m \int_0^{2T} d\tau (A_0(2t - \tau))^2, \quad (13)$$

which leads to

$$D = D_m \int_0^{2T} d\tau (A_0(2t - \tau))^2. \quad (14)$$

In order to connect the GL Hamiltonian with the Monte Carlo results in Ref. 3, we define $\lambda =$ and $\mu_0^2 = -2\nu/\gamma$ and $\lambda = 4g\xi\epsilon D/\gamma^2$ which we calculate by rescaling the ϕ field by $\sqrt{2D\epsilon/\gamma}$. We then calculate the critical point by interpolating the data in Table II which shows the critical bare μ_0^2 value for various λ between 0.01 and 1.

MONTE CARLO DETAILS

We perform a Markov chain Monte Carlo simulation on a 2-dimensional lattice using Glauber dynamics and a global flip $\phi \mapsto -\phi$ after each sweep. To reduce artificial sweeping effects, we use the checkerboard algorithm to order sites. The Glauber dynamics takes one site ϕ_i and considers a new site $\phi'_i = \phi_i + \delta\phi$ where $\delta\phi$ is chosen from a normal distribution with a standard deviation of 2. The change is accepted with a probability

$$P = \left(1 + \exp \left\{ \frac{H[\{\phi'\}] - H[\{\phi\}]}{\epsilon D} \right\} \right)^{-1} \quad (15)$$

where H is the GL Hamiltonian in the main text. We simulate 384 trials with 10^5 sweeps of thermalization and measurements every 101 steps, running for 10^5 sweeps in total.